

Shear Strain Analysis in FSS Microchannel

¹Zaliman Sauli, ¹Vithyacharan Retnasamy, ¹Nor Shakirina Nadzri, ¹Tan Hsio Mei and ²Hussin Kamarudin

¹School of Microelectronic Engineering, Universiti Malaysia Perlis (UniMAP), Pauh Putra Campus, 02600 Arau, Perlis, Malaysia.

²School of Materials Engineering, Kompleks Pusat Pengajian Jejawi 2, Taman Muhibbah, Universiti Malaysia Perlis, 02600 Jejawi, Arau, Perlis, Malaysia.

ARTICLE INFO

Article history:

Received 11 September 2013

Received in revised form 21 November 2013

Accepted 25 November 2013

Available online 5 December 2013

Key words:

Microfluidic; Forward Facing Step; Shear Strain

ABSTRACT

Microfluidics has motivated the development of various fields in biological engineering due to its advantages. The favorable benefits of using microfluidics are being easy to fabricate, requirement of minimal fluid volumes, high-throughput and large scale integration. Microfluidic devices are strongly related with the fluid manipulation. However, the fluids have lack ability to resist deformation therefore the investigation on shear strain rate of fluid flow is required. In this paper, a study on the shear strain rate characteristics in Forward Facing Step (FFS) microchannel was conducted. The shear strain rate was investigated based on different Reynolds (Re) numbers before and after step conditions. The maximum shear strain rate was observed near the wall across the X-axis for both before and after step. Higher Re numbers produced higher shear strain rate distribution.

INTRODUCTION

Microfluidics possesses numerous advantages, including ease to fabricate, reagent consumption reduction, parallel and processing performance enhancement, and large-scale integration [1-4]. Therefore, microfluidics holds great promise to revolutionize various areas of biological engineering, such as cell culture technique [1], point-of-care (POC) diagnostics [5,6] and drug sensitivity testing [7]. Sin, Gao, Liao and Wong (2011) defined microfluidics as a multidisciplinary field investigating the characteristics of small amounts of fluids with length scales from nanometers to micrometers. Since fluids have lack ability to resist deformation, the understanding of shear strain rate of fluid flow behavior is obviously needed. Andre Bakker (2006) stated that strain rate in flow field can be applied for many purposes. For non-Newtonian fluids, the viscosity is mentioned to have strong correlation with the strain rate. In emulsions, droplet size may depend on the strain rate as well. Other than that is the strain rate may affect particle formation and agglomeration in pharmaceutical applications. An article published by Yiping Hong and Fujun Wang (2007) investigated flow rate effect on droplet formation in a co-flowing microfluidic device. Droplet generation in immiscible fluids has been widely used in the field of biology, pharmaceutical, cosmetics and foods. The authors emphasized the strong relation between strain rate and droplet diameter in conjunction with flow rate ratio, Q_d/Q_c . For the case $Q_d/Q_c \geq 0.1$, droplet size is observed to be independent to the flow rate ratio. It is found that a little increase of droplet size may contribute a great significant of strain rate. Hence, a larger size droplet formed with the increase of flow rate ratio will cause an abrupt increase of strain rate which easily leads to disruptive force due to viscosity. Meanwhile, when the $Q_d/Q_c < 0.1$, droplet size is strongly dependent on the flow rate ratio. Xiangdong, Mayur, Maiwenn, Chris, Marc and David (2009) explored the effects of some mechanical features and fluid dynamics on biofluid behavior in microchannel systems. The authors revealed that blood separation application is moving towards new microscopic separation method whereby the shear strain rate is one of the characteristic that plays dominant role in the microchannels. The performance for proposed blood separator was tested for both Newtonian and non-Newtonian flows. Under Newtonian flow, the velocity distribution reflected the difference of the shear strain rate across the channel. The maximum shear strain rate was observed on the boundary layer near the wall region. For the

non-Newtonian flow, the authors summarized that an increase in the input flow rate contributed to the shear strain rate increment within the microchannel system causing a reduction in the viscosity. To the best author's knowledge even though microfluidics research has gained enormous interest currently, there is little work done to investigate further on the strain rate characteristics in microchannels. This motivates us to study detail on the strain rate characteristics in forward facing step (FFS) microchannel. The aim of this paper is to evaluate the effect of different Reynolds (Re) number on the fluid flow behavior before and after the step.

Methodology:

The Ansys software has been used to perform the analysis. Numerical simulations based on Computational Fluid Dynamics (CFD) technologies can provide important insights to determine and enhance the performance of the microfluidic device [11,12]. Fig. 1 showed the computational model with structured mesh of 2560k nodes. A comparison between full part, two parts and five parts has been done to determine the grid independence. Full part for this FFS microchannel produced around 512k nodes. Two parts which the full part microchannel is cut into half and simulated two times yielded $2 \times 512k$ nodes. Meanwhile, five parts whereby the full part microchannel is divided into five parts and simulated five times produced in total nodes of around $5 \times 512k$ nodes. The grid independence was achieved at five parts simulation where the highest nodes were generated. Fluid properties of water with density and viscosity of 997.0479 kg/m^3 and $8.90 \times 10^{-4} \text{ kg/m.s}$ respectively were adapted. Water is an example of the Newtonian fluid which means that it will not change its original fluid state when force acting on it. Laminar flow profile was used for the simulation analysis.

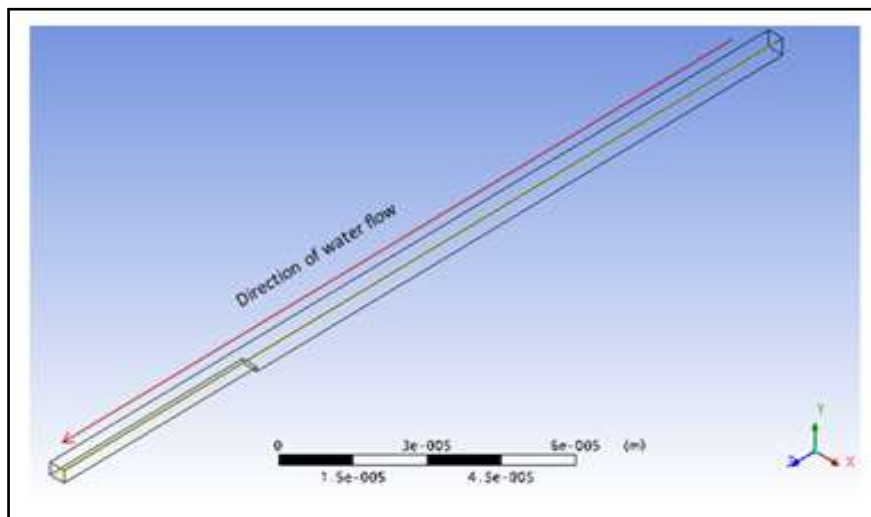


Fig. 1: Computational model analysis of shear strain rate in FFS microchannel.

The length at Z-axis from the inlet channel to the step was $550 \mu\text{m}$ and length from the step to the outlet channel was $450 \mu\text{m}$. Height of the step, H was set as $1 \mu\text{m}$. Fig. 2 illustrated the FFS configuration of this simulation. This square microchannel was designed with dimension of $4 \mu\text{m} \times 4 \mu\text{m}$ inlet channel. The strain rate analysis was evaluated based on six different Re numbers, 0.1, 1, 10, 100, 300 and 500. Observation was concentrated at location $510 \mu\text{m}$ and $590 \mu\text{m}$ from inlet channel which represented the analysis before and after step in the microchannel respectively.

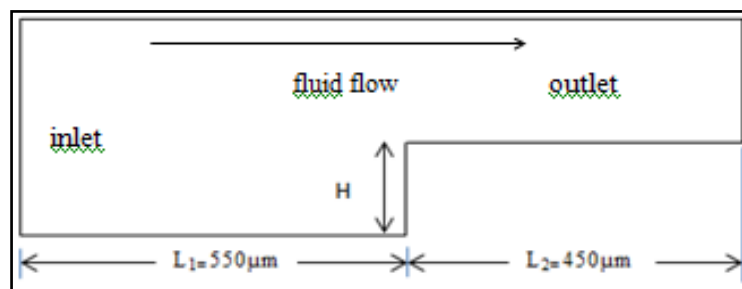


Fig. 2: FFS configuration design.

The different value of Re numbers from 0.1 to 500 altered the inlet velocity as well. Table 1 showed the inlet velocity for each Re numbers used.

Table 1: Inlet Velocity for Reynolds Number 0.1, 1, 10, 100, 300 and 500.

Re number	Inlet velocity /ms ⁻¹
0.1	0.0223
1	0.223
10	2.232
100	22.32
300	66.948
500	111.58

RESULT AND DISCUSSION

The maximum shear strain rate before step was observed to appear near the wall across the x-axis as depicted in Fig. 3. This is caused by the fluid viscous at wall try to stop fluid flowing due to no slip boundary condition. For Newtonian fluid with constant viscosity, the shear strain rate is directly proportional to the velocity flow. Since Re numbers are directly proportional to the fluid velocity, the higher Re numbers were observed to produce higher shear strain rate. At low Re numbers, laminar flow character is dominated.

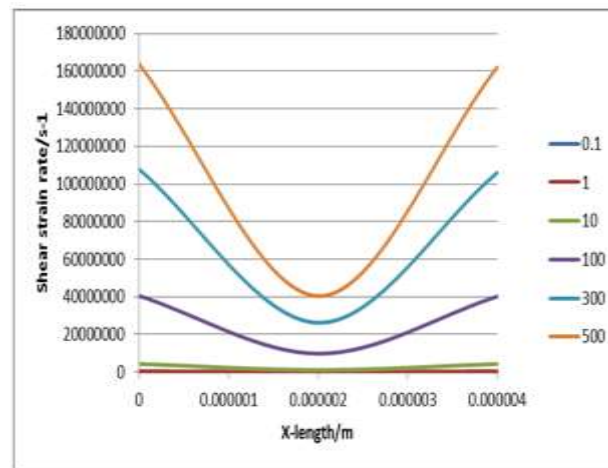


Fig. 3: Shear strain rate before step ($Z=510\mu\text{m}$) with the different Reynolds number.

The analysis after step (at $Z=590\mu\text{m}$) showed similar flow distribution pattern as in Figure 4. Nevertheless, the simulation at $Z=590\mu\text{m}$ exhibited higher shear strain rate near the wall than those simulation at $Z=510\mu\text{m}$. This is due to the narrower channel after the step that causing velocity of the fluid flow was increased after passing through the step.

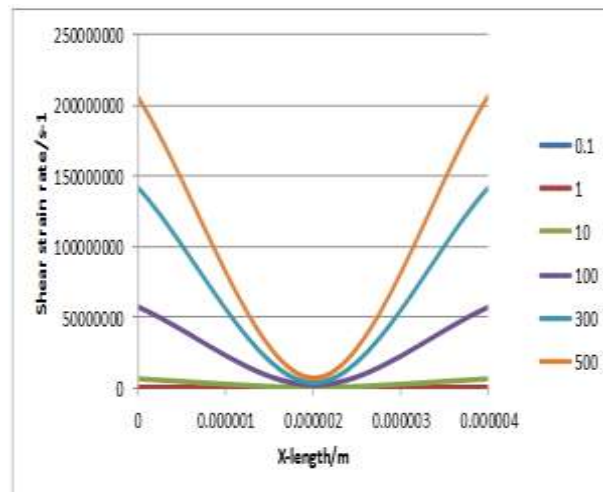


Fig. 4: Shear strain rate after step ($Z=590\mu\text{m}$) with the different Reynolds number.

As a comparison, analysis for both before and after step conditions at $0\mu\text{m}$ (wall) on X-axis was done and the results plotted on the same graph as per Figure 5. Blue line represented before step ($Z=510\mu\text{m}$) and red line represented after step ($Z=590\mu\text{m}$). Due to the increase of fluid velocity after the step, the shear strain rate at $590\mu\text{m}$ was observed higher than at location $510\mu\text{m}$. The shear strain distribution indicated the effect of the Re numbers as well.

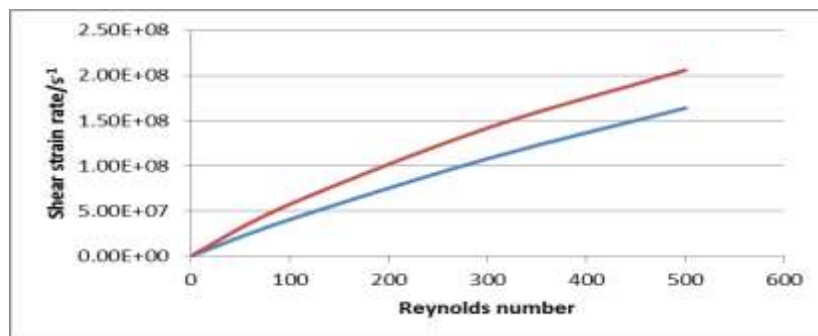


Fig. 5: Shear strain rate at $0\mu\text{m}$ (wall) on X-axis for step height $1\mu\text{m}$ at $Z=510\mu\text{m}$ and $Z=590\mu\text{m}$ with different Reynolds numbers.

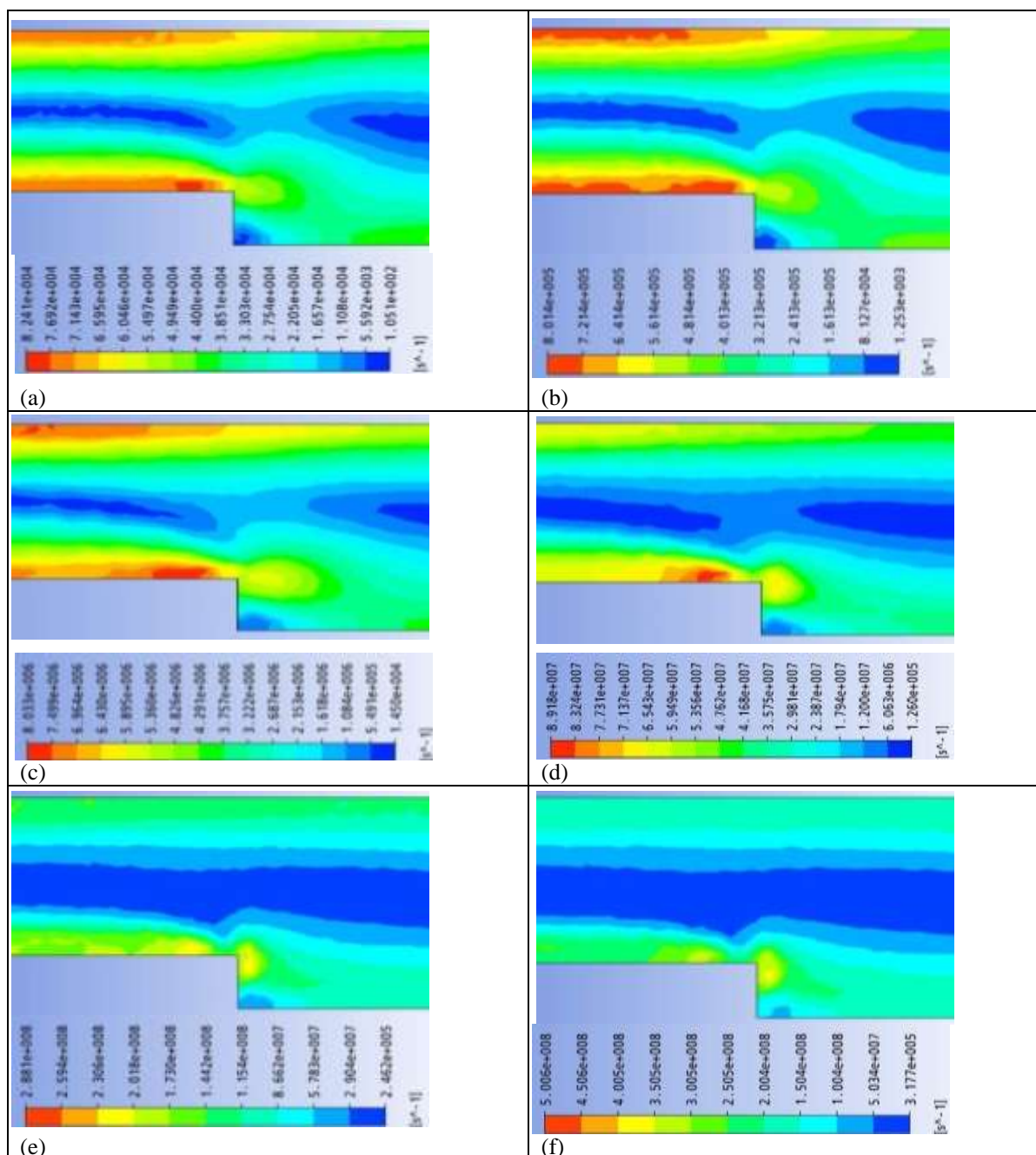


Fig. 6: Shear strain rate contour for step height $1\mu\text{m}$ with different Reynolds Number (a) Re 0.1, (b) Re 1, (c) Re 10, (d) Re 100, (e) Re 300 and (f) Re 500

Figure 6 (a-f) illustrated the shear strain rate contour for all Re numbers used. We observed that blue color represented the lowest rate of shear strain and visibly dominated at the center of the microchannel for all Re numbers. On the other hand, the maximum shear strain rate occurred near the wall region and getting higher after passing through the step. From Figure 6(a), the red color appeared close to the wall region after fluid flowing through the narrower cross section area. So, the highest shear strain rate for Re 0.1 is 82.41 k s^{-1} . Same simulation result obtained for Re 1, 10 and 100 depicted in Figure 6(b), (c) and (d) whereby the highest rate of shear strain represented by red color contour. Meanwhile, the highest shear strain rate for Re 300 and 500 can be seen by yellow color contour existed near the step as in Figure 6(e) and (f). Re 500 obviously exhibited the highest value of shear strain rate followed by Re 300, 100, 10, 1 and 0.1.

Conclusion:

The shear strain rate characteristics of forward facing step microchannel have been investigated. Simulation at $Z=590 \mu\text{m}$ exhibited higher shear strain rate near the wall than simulation at $Z=510 \mu\text{m}$ due to reduction of cross section area after the step. The maximum rate of shear strain achieved near the wall of the microchannel, while the minimum shear strain rate was observed at the center of the channel. Varied Re numbers were found to influence the shear strain distribution of the fluid flow. Higher Re numbers produced higher shear strain rate for both before and after step conditions.

ACKNOWLEDGEMENT

The authors would like to thank and acknowledge the School of Microelectronic Engineering, Universiti Malaysia Perlis for their support and facility. The authors appreciation are extended to the Ministry of Higher Education for the support given.

REFERENCES

- [1] Dan Gao, 2012. Hongxia Liu, Yuyang Jiang and Jin-Ming Lin, "Recent developments in microfluidic devices for in vitro cell culture for cell-biology research," Trends in Analytical Chemistry, 35.
- [2] Liu Wen-Ming, Li Li, Ren Li, Wang Jian-Chun, Tu Qin, Wang Xue-Qin, Wang Jin-Yi, 2012. "Diversification of Microfluidic Chip for Applications in Cell-Based Bioanalysis, Chinese Journal Of Analytical Chemistry, 40(1).
- [3] Yegermal T. Atalay, Steven Vermeir, Daan Witters, Nicolas Vergauwe, Bert Verbruggen, Pieter Verboven, Bart M. Nicolai and Jeroen Lammertyn, 2011. "Microfluidic analytical systems for food analysis," Trends in Food Science & Technology, 22.
- [4] Saurabh Vyawahare, Andrew D. Griffiths and Christoph A. Merten, 2010. "Miniaturization and Parallelization of Biological and Chemical Assays in Microfluidic Devices," Chemistry & Biology Review.
- [5] Farhan Ahmad and Syed A. Hashsham, 2012. "Miniaturized nucleic acid amplification systems for rapid and point-of-care diagnostics: A review," Analytica Chimica Acta 733.
- [6] Mandy L.Y. Sin, Jian Gao, Joseph C. Liao and Pak Kin Wong, 2011. "System Integration - A Major Step toward Lab on a Chip," Journal of Biological Engineering.
- [7] Zhiyun Xu, Yanghui Gao, Yuanyuan Hao, Encheng Li, Yan Wang, Jianing Zhang, Wenxin Wang, Zhancheng Gao and Qi Wang, 2013. "Application of a microfluidic chip-based 3D co-culture to test drug sensitivity for individualized treatment of lung cancer," Biomaterials, 34.
- [8] Andre Bakker, 2006. "Applied Computational Fluid Dynamics," Computational Fluid Dynamic, Eng 150
- [9] Yiping Hong and Fujun Wang, 2007. "Flow rate effect on droplet control in a co-flowing microfluidic device," Microfluid Nanofluid.
- [10] Xiangdong Xue, Mayur K. Patel, Maiwenn Kersaudy-Kerhoas, Chris Bailey, Marc P.Y. Desmulliez and David Topham, 2009. "Effect of Fluid Dynamics and Device Mechanism on Biofluid Behaviour in Microchannel Systems: Modelling Biofluids in a Microchannel Biochip Separator," International Conference on Electronic Packaging Technology & High Density Packaging.
- [11] Manguo Huang, Shangchun Fan, Weiwei Xing and Changting Liu, 2010. "Microfluidic cell culture system studies and computational fluid dynamics," Mathematical and Computer Modelling, 52.
- [12] Xiangdong Xue, Mayur K. Patel, Maiwenn Kersaudy-Kerhoas, Marc P.Y. Desmulliez, Chris Bailey and David Topham, 2012. "Analysis of fluid separation in microfluidic T-channels.